



# Harmonic wavelet-based data filtering for enhanced machine defect identification

Ruqiang Yan<sup>a,\*</sup>, Robert X. Gao<sup>b</sup>

<sup>a</sup> School of Instrument Science and Engineering, Southeast University, Nanjing, Jiangsu 210096, China

<sup>b</sup> Department of Mechanical Engineering, University of Connecticut, Storrs, CT 06269, USA

## ARTICLE INFO

### Article history:

Received 26 May 2009

Received in revised form

2 February 2010

Accepted 4 February 2010

Handling Editor: K. Shin

Available online 26 February 2010

## ABSTRACT

A filter construction technique is presented for enhanced defect identification in rotary machine systems. Based on the generalized harmonic wavelet transform, a series of sub-frequency band wavelet coefficients are constructed by choosing different harmonic wavelet parameter pairs. The energy and entropy associated with each sub-frequency band are then calculated. The filtered signal is obtained by choosing the wavelet coefficients whose corresponding sub-frequency band has the maximum energy-to-entropy ratio. Experimental studies using rolling bearings that contain different types of structural defects have confirmed that the developed new technique enables high signal-to-noise ratio for effective machine defect identification.

© 2010 Elsevier Ltd. All rights reserved.

## 1. Introduction

Recent advancement of miniaturized sensor design and wireless data communication has led to an increasing number of sensors to be installed on machine systems and civil structure for comprehensive and timely gathering of data to monitor the condition of the system in real-time. High quality data acquisition requires both proper sensor placement (such that sensor locations provide for adequate coverage of signal features while minimizing structural repercussion [1,2]), and effective extraction of characteristic features from the sensor data to reliably diagnose the current working state of the system [3,4]. Of the various signals commonly analyzed for monitoring and diagnosis purposes (e.g. vibration, acoustic emission, temperature, force and torque variations), vibration signals measured from a machine contain rich physical information about the condition status of the machine. Proper analysis of such signals is a critical prerequisite for clear identification of the hidden defect and timely diagnosis of potential machine failure [5,6].

As a signal analysis tool, the wavelet transform (WT) has the ability to provide both the time domain and the frequency domain information of the signal simultaneously through a series of convolution operations between the signal being analyzed and the base wavelet under different scaling parameters. Such adaptivity makes it better suited for analyzing non-stationary signals [7,8], which is often encountered in rotary machines such as seen in vibrations measured on machine tools during the metal removing process [9], as compared to the commonly used spectral analysis technique. Of the various types of wavelets developed over the past decades, the harmonic wavelet possesses compact frequency expression [10], thus can be efficiently implemented through a pair of Fourier and inverse Fourier transform operations. Such feature made it well suited for dynamic modeling of the Burgers equation [11], non-linear partial differential equation solutions [12], heart rate variability analysis [13], particle shape pattern recognition [14], image denoising [15], and surface

\* Corresponding author.

E-mail addresses: [ruqiang@seu.edu.cn](mailto:ruqiang@seu.edu.cn) (R. Yan), [rgao@engr.uconn.edu](mailto:rgao@engr.uconn.edu) (R.X. Gao).

electromyographic (EMG) signal classification [16]. An overview of applying harmonic wavelet transform for vibration signal analysis was provided in [17], and examples have included vibration analysis of buildings [17], beam structure [18], rotary machines [19], rotor rig testing systems [20,21], helicopter gearbox [22], and rolling bearings [23].

In addition to efficient algorithm implementation, which has attracted significant efforts from various researchers, the harmonic wavelet can also be considered as an ideal signal filter, because of its box-shaped spectrum characteristic (i.e. the magnitude of the spectrum is zero except for a certain range of frequency components) [10]. Such characteristic motivates this study, which is focused on the filtering aspect of the harmonic wavelet. Specifically, a harmonic wavelet filtering approach for enhanced defect identification in rotary machines has been developed. After introducing the theoretical basis of the harmonic wavelet transform in Section 2, the approach using the energy-to-entropy ratio criterion for tuning the parameter pair of the harmonic wavelet filter is discussed in Section 3. Then a synthetic signal based on impulse response of a rolling bearing is formulated to evaluate the performance of the presented wavelet filter. Section 4 describes experimental studies of rolling bearings that contain different types of structural defects to evaluate the filtering technique. Finally, conclusions are drawn in Section 5.

**2. Theoretical framework**

The wavelet transform decomposes a signal  $x(t)$  onto a time-scale plane through a series of convolution operations between the signal and a selected base wavelet [8]:

$$a(s, t) = |s|^{-1/2} \int_{-\infty}^{\infty} x(\tau) \overline{\psi}\left(\frac{\tau-t}{s}\right) d\tau \tag{1}$$

where  $\overline{\psi}(\cdot)$  is the complex conjugate of the scaled and shifted base wavelet  $\psi(\cdot)$ . Given that the convolution operation in one domain equals point-wise multiplication in another domain [24],  $a(s,t)$  in Eq. (1) can be alternatively calculated as

$$a(s, t) = F^{-1}\{A(s, f)\} = |s|^{1/2} F^{-1}\{X(f) \overline{\Psi}(sf)\} \tag{2}$$

where  $X(f)$  and  $\overline{\Psi}(\cdot)$  denote the Fourier transform of  $x(t)$  and  $\overline{\psi}(\cdot)$ , respectively. The symbol  $F^{-1}$  denotes the inverse Fourier transform. Fig. 1 illustrates the calculation procedure of wavelet transform.

Of the various wavelets developed over the past decades, the harmonic wavelet is characterized by the simplicity of its expression in the frequency domain, defined as [25,26]

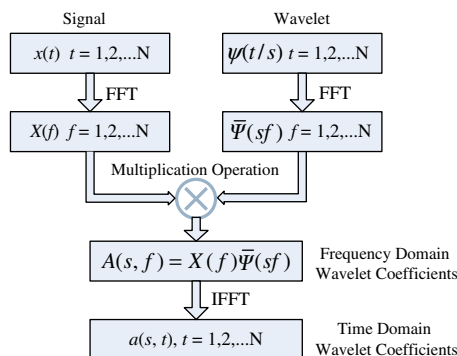
$$\Psi_{m,n}(f) = \begin{cases} \frac{1}{n-m} & m \leq f < n \\ 0 & \text{else where} \end{cases} \tag{3}$$

Here the parameter pair  $(m, n)$  specifies the lower and upper cutoff frequencies of the frequency band defined by the harmonic wavelets, instead of the scale parameter  $s$  as commonly used in Eqs. (1) and (2). Furthermore, the symbols  $m$  and  $n$  are both real but not necessarily integers, thus can be used to define an arbitrary frequency band, in which the center frequency  $f_c$  and bandwidth  $f_{BW}$  of the harmonic wavelet are defined as

$$\begin{cases} f_c = (m+n)/2 \\ f_{BW} = n-m \end{cases} \tag{4}$$

Correspondingly, the harmonic wavelet expression in time domain is expressed as

$$\psi_{m,n}(t) = \frac{e^{jn2\pi t} - e^{jm2\pi t}}{j2\pi(n-m)t} \tag{5}$$



**Fig. 1.** Procedure of wavelet transform.

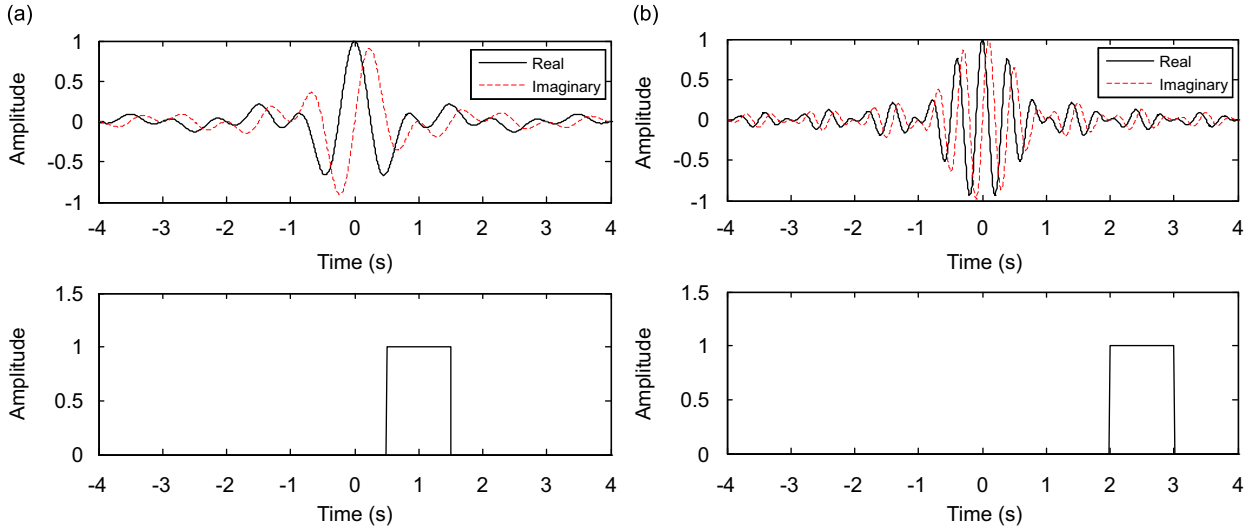


Fig. 2. Harmonic wavelet with different parameter pairs  $(m, n)$ : (a) parameter pair  $(0.5, 1.5)$  and (b) parameter pair  $(2, 3)$ .

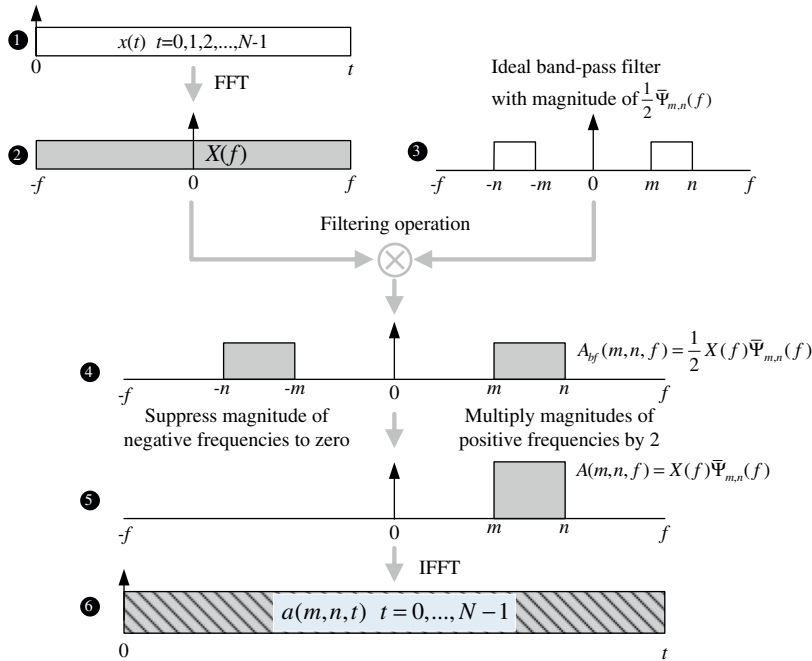


Fig. 3. Schematic diagram of modified band-pass filtering. ① signal  $x(t)$ ; ②  $X(f)$ : Fourier transform results of  $x(t)$ ; ③ Ideal band-pass filter with magnitude of  $(1/2)(n - m)$  and band-pass  $m \leq f < n$ ; ④  $A_{bf}(m, n, f)$ : Output of the ideal band-pass filtering operation in frequency domain; ⑤  $A(m, n, f)$ : Equivalent results of the harmonic wavelet coefficients in frequency domain; ⑥  $a(m, n, t)$ : harmonic wavelet coefficients in time domain.

Fig. 2 illustrates the harmonic wavelet with two exemplary parameter pairs  $(0.5, 1.5)$  and  $(2, 3)$ , in which the bandwidth and magnitude are same for the two parameter pairs. It is seen that through variation of the center frequency and bandwidth, the harmonic wavelet can be scaled to match a signal in different frequency regions, thus realizing the function of signal filtering.

Eq. (5) implies the phase difference between the real part of the harmonic wavelet and its imaginary part is equal to  $90^\circ$ . This means the phase of a signal remains unchanged after the harmonic wavelet transform of the signal was performed. As an example, when the signal  $x(t) = \cos(2\pi f_1 t + \theta)$  is decomposed by a harmonic wavelet transform, the wavelet coefficients:

$$a(m, n, t) = |n - m|^{1/2} F^{-1} \{ X(f) \bar{\Psi}_{m,n}(f) \} = |n - m|^{1/2} F^{-1} \left\{ \pi [e^{-i\theta} \delta(2\pi f + 2\pi f_1) + e^{i\theta} \delta(2\pi f - 2\pi f_1)] \frac{1}{n - m} \right\} = \frac{e^{i(2\pi f_1 t + \theta)}}{4\pi |n - m|^{1/2}} \quad (6)$$

have the same phase  $\theta$  as that of the original signal. Such property makes the harmonic wavelet an ideal band-pass filter.

To illustrate the functionality of the harmonic wavelet as an ideal filter, a schematic diagram of modified band-pass filtering is given in Fig. 3.

As shown in Fig. 3, after taking the Fourier transform of the signal  $x(t)$  to obtain its frequency expression  $X(f)$ , a band-pass filtering operation (the magnitude of the ideal band-pass filter is  $(1/2)(1/(n-m))$ ), and the pass-band is  $m \leq |f| \leq n$  is performed to obtain the filtered signal spectrum  $A_{bf}(m, n, f)$ , which can be expressed as

$$A_{bf}(m, n, f) = \frac{1}{2\pi} \int_{-\infty}^{\infty} a_{bf}(m, n, t) e^{-j2\pi ft} dt = \begin{cases} X(f) \frac{1}{2} \frac{1}{n-m}, & m \leq |f| < n, \\ 0, & \text{otherwise} \end{cases} \quad (7)$$

In Eq. (7),  $a_{bf}(m, n, t)$  is the filtered signal resulting from the ideal band-pass filtering operation. By suppressing magnitude of the negative frequency components to zero and multiplying magnitude of the positive frequency components by 2, the result  $A(m, n, f)$  can be expressed as

$$A(m, n, f) = \begin{cases} 2A_{bf}(m, n, f), & f \geq 0, \\ 0, & f < 0 \end{cases} = \begin{cases} X(f) \frac{1}{n-m}, & f \geq 0, \\ 0, & f < 0 \end{cases} \quad (8)$$

This is equivalent to the coefficients of the harmonic wavelet transform in the frequency domain. Taking the inverse Fourier transform of  $A(m, n, f)$  results in:

$$\begin{aligned} a(m, n, t) &= \int_{-\infty}^{\infty} A(m, n, f) e^{j2\pi ft} df = \int_0^{\infty} 2A_{bf}(m, n, f) e^{j2\pi ft} df \\ &= \int_0^{\infty} 2 \left[ \frac{1}{2\pi} \int_{-\infty}^{\infty} a_{bf}(m, n, \tau) e^{-j2\pi f\tau} d\tau \right] e^{j2\pi ft} df \\ &= \frac{1}{\pi} \int_0^{\infty} \int_{-\infty}^{\infty} a_{bf}(m, n, \tau) e^{j2\pi f(t-\tau)} d\tau df \end{aligned} \quad (9)$$

It is noted that  $\int_0^{\infty} e^{j2\pi ft} df = \pi \delta(t) + j/t$ , where  $\delta(t)$  is the delta function. Accordingly, Eq. (9) can be expressed as

$$a(m, n, t) = a_{bf}(m, n, t) + \frac{j}{\pi} \int_{-\infty}^{\infty} \frac{a_{bf}(m, n, \tau)}{t-\tau} d\tau = a_{bf}(m, n, t) + jH[a_{bf}(m, n, t)] \quad (10)$$

where  $H[\cdot]$  represents the Hilbert transform operation. Eq. (10) indicates the real part of  $a(m, n, t)$  is the filtered signal of an ideal band-pass filtering operation. This means that an ideal band-pass filter can be realized through harmonic wavelet transform, making it an effective tool for noises suppression and feature extraction.

### 3. Harmonic wavelet filtering

When a structural defect occurs on the surface of a rotary machine component, defect-induced resonant vibration (which is non-stationary in nature and within high frequency region) will be generated and mixed with those from other vibration sources. To improve the signal-to-noise ratio for effective defect identification, vibration signals need to be filtered first before analyzed. As presented above, the harmonic wavelet transform provides an effective tool for this purpose. Theoretically, the center frequency of the harmonic wavelet derived from the selected parameter pair  $(m, n)$  should match that of the defect-related vibration, in order to best extract the defect features out of the measured vibration signal. It follows that a harmonic wavelet filter can be constructed by tuning the parameter pair  $(m, n)$ . In this study, a criterion that accounts for the energy-to-entropy ratio of the harmonic wavelet coefficients is proposed to achieve effective signal filtering.

#### 3.1. Parameter tuning criterion

The energy content of a vibration signal measured on a rotary machine is directly related to the degree of severity of the defect condition. Thus energy can be utilized as a measure for selecting the parameter pair  $(m, n)$ . The amount of energy contained in the signal  $x(t)$  is calculated as

$$E_{\text{energy}} = \sum_{t=1}^N |x(t)|^2 \quad (11)$$

where  $N$  is the length of the signal measured by the number of data points, and  $|x(t)|$  is the amplitude of the signal. Based on the Parseval theory, the energy content of the signal can also be calculated from its wavelet coefficients expressed as

$$E_{\text{energy}} = \sum_{m, n} \sum_{t=1}^N |a(m, n, t)|^2 \quad (12)$$

Eq. (12) indicates that the energy associated with a particular parameter pair  $(m, n)$  can be quantified as

$$E_{\text{energy}}(m, n) = \sum_{t=1}^N |a(m, n, t)|^2 \quad (13)$$

Given that for the same amount of energy associated with a particular parameter pair, the specific condition of the signal may be different (e.g., a spectrum with few concentrated frequency components of high magnitudes vs. a widespread spectrum), the spectral distribution of the energy needs also to be considered to ensure effective extraction of the defect-related vibration. The energy distribution of the wavelet coefficients is quantitatively described by the Shannon entropy as [27]

$$E_{\text{entropy}}(m, n) = - \sum_{i=1}^N p_i \log_2 p_i \quad (14)$$

where  $p_i$  is the energy probability distribution of the wavelet coefficients, defined as

$$p_i = \frac{|a(m, n, i)|^2}{E_{\text{energy}}(m, n)} \quad (15)$$

with  $\sum_{i=1}^N p_i = 1$ , and  $p_i \log_2 p_i = 0$  if  $p_i = 0$ .

Eqs. (14) and (15) indicate that the entropy of the wavelet coefficients is bounded by

$$0 \leq E_{\text{entropy}}(m, n) \leq \log_2 N \quad (16)$$

where  $E_{\text{entropy}}(m, n)$  will be equal to

- (1) Zero, if all other wavelet coefficients are equal to zero except for one wavelet coefficient, or
- (2)  $\log_2 N$ , if the probability of energy distribution for all the wavelet coefficients are the same, i.e.  $1/N$ .

This leads to the conclusion that the lower the entropy value is, the higher the energy concentration will be. As a result, the energy and Shannon entropy content of a signal's wavelet coefficients can be used to tune the parameter pair for construction of the wavelet filter. The selected parameter pair should guarantee that the maximum amount of energy of the defect-related vibration can be extracted while minimizing the Shannon entropy of the corresponding wavelet coefficients. A combination of the energy and Shannon entropy content of a signal's wavelet transform coefficients, denoted as energy-to-entropy ratio, is thus designed as

$$\rho(m, n) = \frac{E_{\text{energy}}(m, n)}{E_{\text{entropy}}(m, n)} \quad (17)$$

where the energy  $E_{\text{energy}}(m, n)$  and the entropy  $E_{\text{entropy}}(m, n)$  are calculated using Eqs. (13) and (14), respectively. Accordingly, the parameter pair can be selected by maximizing the energy-to-entropy ratio  $\rho(m, n)$ , which leads to the following criterion

**Maximum energy-to-entropy ratio criterion:** The parameter pair  $(m, n)$ , whose corresponding wavelet coefficients has produced the maximum energy-to-entropy ratio, should be chosen to construct the wavelet filter for defect-related feature extraction.

Based on the above criterion, the procedure for realizing the harmonic wavelet filtering algorithm is shown in Fig. 4. Specifically, the input signal is first decomposed by the harmonic wavelet transform, and a series of wavelet coefficients with different parameter pairs were obtained. The corresponding energy and Shannon entropy content for each parameter pair are then calculated to formulate the energy-to-entropy ratio matrix. The parameter pair, whose corresponding wavelet coefficients possess the highest energy-to-entropy ratio, is subsequently chosen to construct the wavelet filter.

Theoretically, any parameter pair  $(m, n)$  can be chosen as the potential candidate for constructing the harmonic wavelet filter, as long as the condition  $0 < m < n \leq f_s/2$  is met, where  $f_s$  is the data sampling rate. This translates into a total of  $C_{N/2}^2 = (N/2)(N/2-1)/2$  parameter pairs, with  $N$  being the total number of data points. For each pair of Fourier and inverse Fourier transforms, the total number of operations needed can be calculated as  $8N \log_2(N)$  [28]. When the energy-to-entropy ratio criterion is applied to conducting an exhaustive search through all the possible parameter pairs of  $(m, n)$ , significant computational cost may result. Specifically, the magnitude of the computational complexity can be approximated using the big O notation as  $O(N^3 \log_2(N))$  [29]. In practical applications, such computational complexity may be reduced to  $O(N^2 \log_2(N))$  when a fixed bandwidth  $(n-m)$  is chosen. Such a reduction leads to a decrease of the number of parameter pairs from  $(N/2)(N/2-1)/2$  to  $(N/2-1)$ . As an example, for bearing defect identification, the frequency range can be reduced from  $[0, f_s/2]$  to  $[10f_{\text{rev}/\text{min}}, f_s/2]$  Hz, where  $f_{\text{rev}/\text{min}}$  is the shaft rotating speed and  $f_s$  is the sampling rate. The lower bound of  $10f_{\text{rev}/\text{min}}$  Hz is chosen to minimize influence from the shaft harmonics, unbalance, and misalignment. The bandwidth of the harmonic wavelet is generally fixed at about 10 times of the defect-induced repetitive frequency  $f_d$  to ensure enough signal energy to be covered in the filtered signal. This requires that the selection of parameter pair should satisfy the condition of  $(n-m) = 10f_d$ , leading to a decrease of the parameter pairs. It should be noted that the initial condition parameters (e.g., frequency range  $[10f_{\text{rev}/\text{min}}, f_s/2]$ , and bandwidth  $10f_d$ ) can be obtained from the

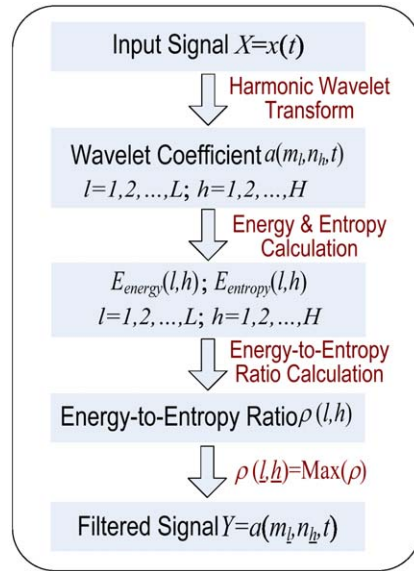


Fig. 4. Illustration of the harmonic wavelet filtering algorithm.

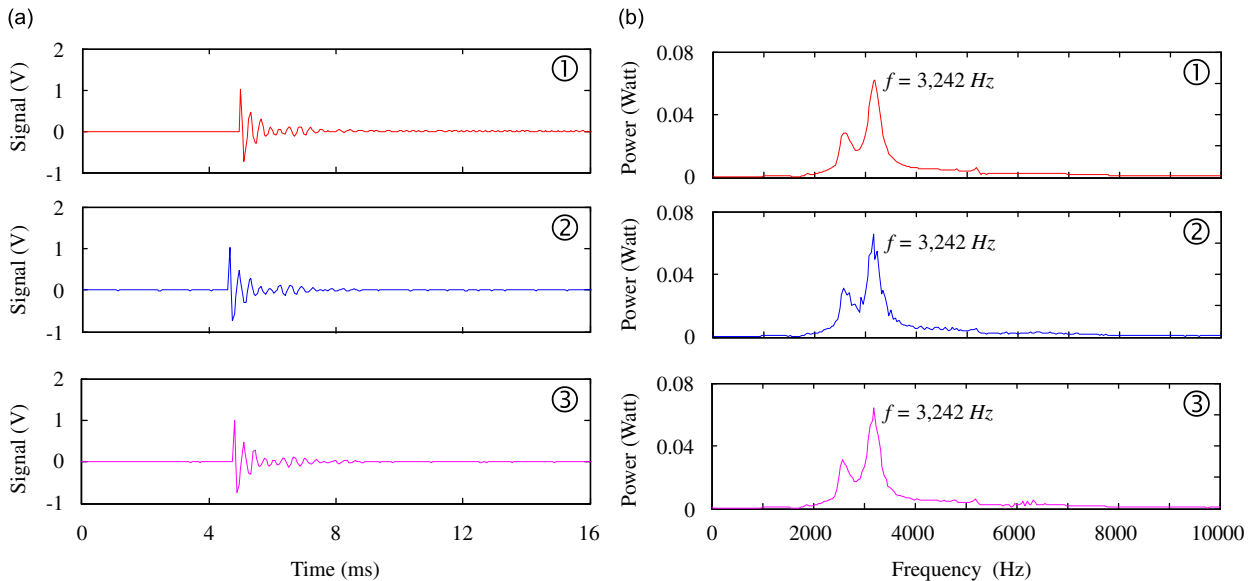


Fig. 5. Impulse responses measured on a ball bearing (model 2214).

rotating speed and geometry of the bearing. Once the initial condition parameters are determined, the selection of parameter pair  $(m, n)$  for harmonic wavelet filter construction can be performed automatically without intervention from the user.

### 3.2. Numerical evaluation

To evaluate the performance of the presented harmonic wavelet filtering technique, a synthetic signal was first constructed from the actual impulse response of a bearing test system, with additive white noise. Fig. 5 illustrates three impulse responses of a ball bearing (model 2214) from an impact test, with the sampling frequency being 20 kHz. The dominant frequency component of the signal was identified to be 3242 Hz. This frequency component was considered as one of the intrinsic frequency components existing in the bearing test system, and would be excited by bearing defect-related impacts.

Given the cyclic nature of vibration signals associated with the rotary machine, the impacts occur on the bearing at a constant time interval. The impact-induced vibrations can be modeled as  $x(t) = \sum_i A_i \delta(t-iT) \otimes h(t)$  [30], where the symbol  $\otimes$  denotes convolution operation,  $A_i$  represents the magnitude of the  $i$ th impulse. The interval  $T$  between the two consecutive impulses is determined by the rotating speed and geometry of the test bearing. The term  $h(t)$  is the impulse response of the bearing test system, as shown in Fig. 5. By adding the white noise, which emulates other structural-borne vibration and environmental noise, a synthetic signal  $y(t)$  simulating the actual bearing vibration signal was generated as  $y(t)=x(t)+e(t)$  with  $e(t)$  being the noise. The procedure on how the synthetic signal was constructed is shown in Fig. 6. In this study, the bearing was assumed to have a localized defect on the outer raceway (i.e.  $A_i$  is a constant) and runs at 600 rev/min. This means 16 defect-induced impacts will be generated per revolution, which translates into an impulse response interval  $T$  of 12.5 ms, or an impact repetition frequency of 80 Hz.

Fig. 7 illustrates the synthetic signal corrupted by the white noise, with the signal-to-noise ratio being  $-12$  dB. Harmonic wavelet transform was applied to the signal over the frequency range [100, 10,000] Hz with the bandwidth of the harmonic wavelet being selected as 800 Hz. Then the energy-to-entropy ratios at different center frequencies were calculated. The results shown in Fig. 8 indicates that the harmonic wavelet with center frequency at 3240 Hz and bandwidth at 800 Hz have produced the highest energy-to-entropy ratio. Based on Eq. (5), the corresponding parameter pair (2840, 3640) Hz was thus chosen to construct the wavelet filter to analyze the synthetic signal. The filtered signal is illustrated in Fig. 9, and the impulse responses with 12.5 ms time interval were clearly identified, confirming the effectiveness of the harmonic wavelet filtering.

To evaluate the effectiveness of the harmonic wavelet filter, the synthetic signal was also processed using the traditional band-pass filter. Of various types of band-pass filters (i.e., Butterworth, Chebyshev, and elliptic, etc.), the Butterworth filter was chosen, since it is designed to have a frequency response as flat as possible in the pass-band [31]. This leads to a higher level of similarity with the harmonic wavelet filter than other types of filters. Fig. 10 illustrates the filtered results using Butterworth filter at order 6, which has the same bandwidth as that of the harmonic wavelet filter. It is seen that the impact interval of 12.5 ms was also identified when the bandwidth of the Butterworth filter was chosen

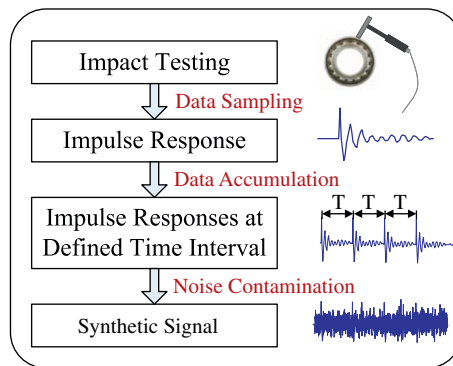


Fig. 6. Procedure of synthetic signal formulation.

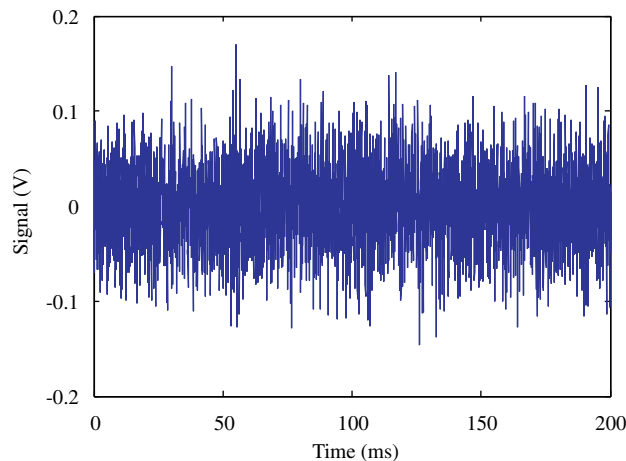
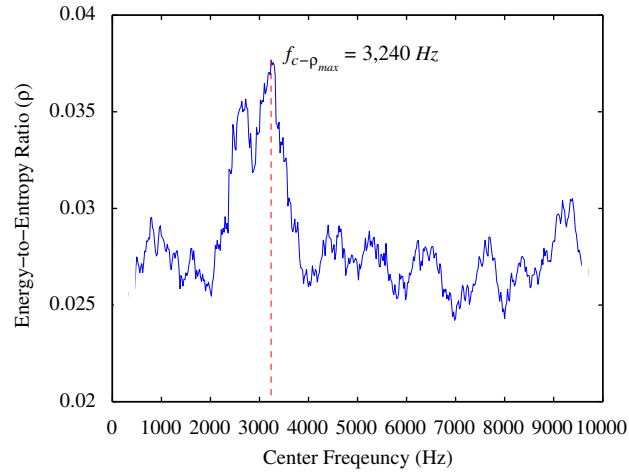
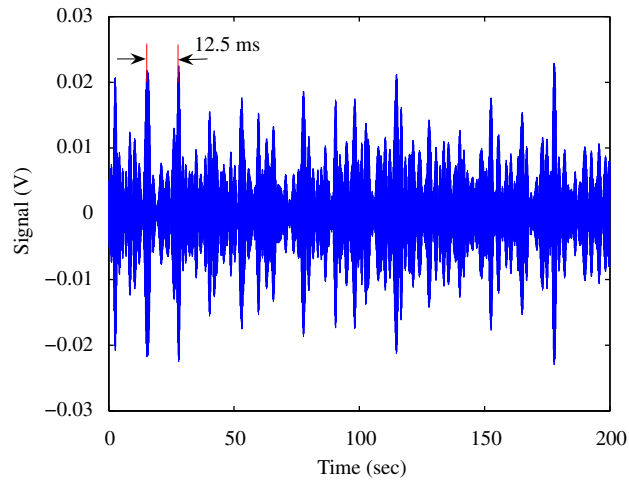


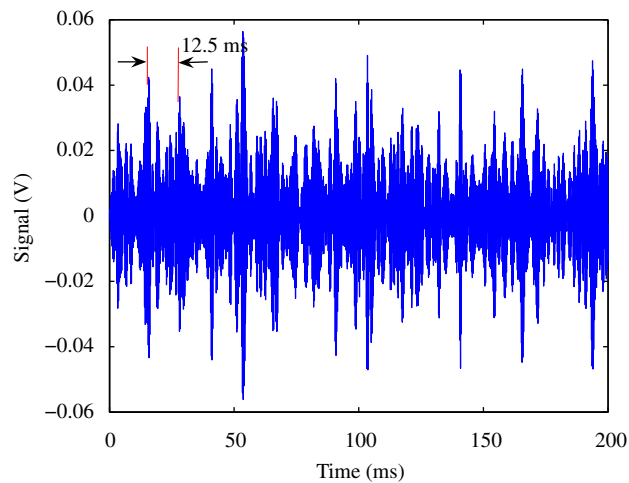
Fig. 7. Synthetic signal (SNR =  $-12$  dB).



**Fig. 8.** Energy-to-entropy ratio vs. center frequency.




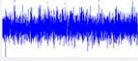
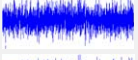

**Fig. 9.** Filtered signal using harmonic wavelet at parameter pair (2840, 3640) Hz.

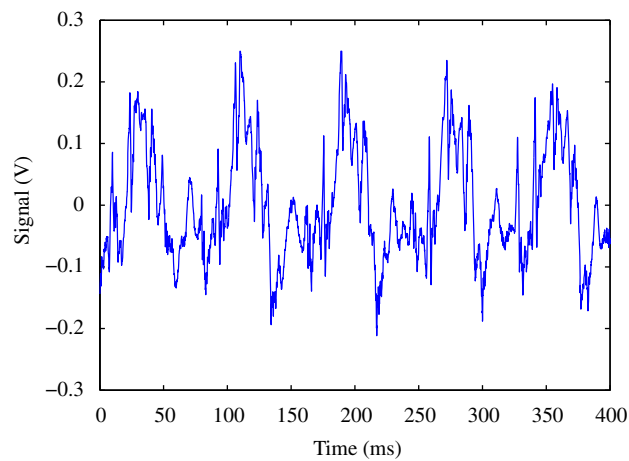


**Fig. 10.** Filtered signal using Butterworth filter at order 6.



**Table 1**  
Comparison results under different SNRs.

Synthetic signal		Filtering operation	
Waveform	(dB)	Butterworth filter (dB)	Wavelet filter (dB)
	-8	-0.5	0.2
	-10	-2.5	-1.8
	-12	-4.5	-3.8
	-14	-6.5	-5.8



**Fig. 11.** Signal measured from a type 6220 ball bearing.

appropriately. To quantitatively compare the two filtering techniques, the signal-to-noise ratio of the filtered signal was calculated. It was found that the harmonic wavelet filter provided a higher signal-to-noise ratio ( $-3.8$  dB) than that of the Butterworth filter ( $-4.5$  dB). This is because the Butterworth filter only separates signals within the pass-band from the rest of other frequency band components, while the harmonic wavelet filter can further improve the signal-to-noise ratio within the pass-band by its nature of operation, i.e., extracting the impulsive vibration component while simultaneously suppressing other components within the pass-band.

To evaluate the robustness of the harmonic wavelet filtering technique, additional synthetic signals with different signal-to-noise ratios were constructed and processed. The results shown in Table 1 demonstrate that harmonic wavelet filtering technique provides consistently better performance than the traditional band-pass filtering technique.

#### 4. Experimental verification

The harmonic wavelet filtering technique was further evaluated experimentally using realistic signals measured from bearings with localized defects. Details are described below.

##### 4.1. Inner raceway defect identification

The first experiment was conducted on a ball bearing (type 6220, outer diameter 180 mm) with a 0.25 mm hole on its inner raceway. The bearing was run at 740 rev/min, and vibration was measured by an accelerometer at the sampling frequency of 10 kHz, as shown in Fig. 11.

Applying the harmonic wavelet transform to the signal decomposed it into different sub-frequency bands. Then the energy-to-entropy ratio for each of the sub-frequency bands was calculated. As shown in Fig. 12, the sub-frequency band

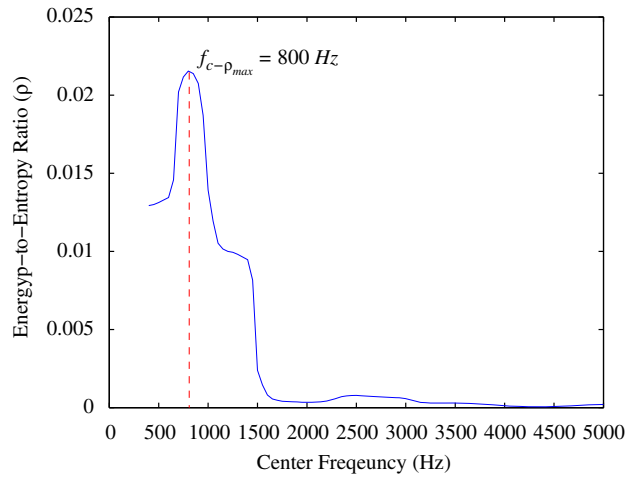


Fig. 12. Energy-to-entropy ratio vs. center frequency.

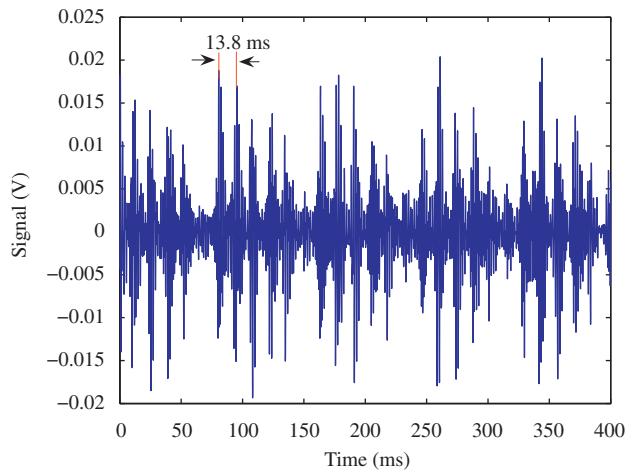


Fig. 13. Filtered results of the bearing vibration signal with harmonic wavelet parameter pair of (400, 1200)Hz.

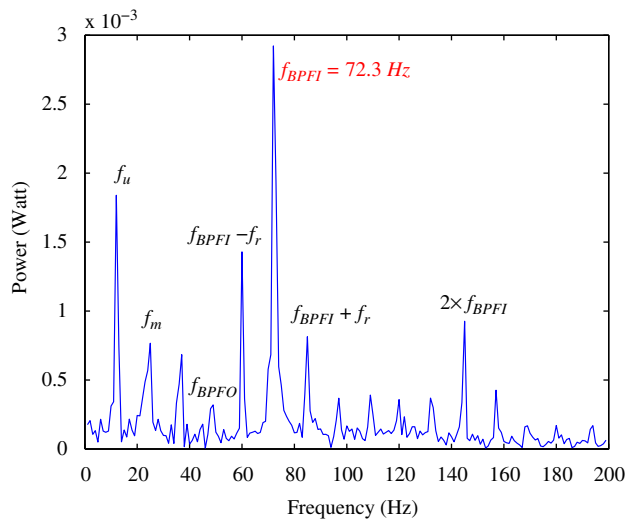


Fig. 14. Enveloping spectrum of the filtered bearing vibration signal with harmonic wavelet parameter pair of (400, 1200)Hz.

with the center frequency at 800Hz possesses the highest energy-to-entropy ratio. Subsequently, the corresponding parameter pair (400, 1200)Hz was chosen to construct the harmonic wavelet filter. The waveform of the filtered signal is shown in Fig. 13, where an impact interval of 13.8 ms was identified. Such an interval matches the  $f_{BPFI}=72.3$  Hz frequency characteristics, thus reveals the existence of the inner raceway defect.

This conclusion was verified by the enveloping spectrum of the filtered vibration signal as shown in Fig. 14. It is also noted that frequency components at 60 and 84.6 Hz were also identified in Fig. 14, which reflects upon the combined effect of bearing rotation (12.3 Hz) and structural defect (72.3 Hz).

For purpose of comparison, another parameter pair (800, 1600)Hz of the harmonic wavelet was used to filter the bearing vibration signal. Although the impact interval of 13.8 ms (Fig. 15) could be identified from the filtered signal, the defect pattern was not as clear as that shown in Fig. 13. This is verified by its corresponding enveloping spectrum as shown in Fig. 16, where the magnitude (2.28 mW) of the 72.3 Hz frequency characteristics is lower than that (2.93 mV) shown in Fig. 14. It thus demonstrated the effectiveness of the parameter tuning criterion for designing the harmonic wavelet filter.

#### 4.2. Outer raceway defect identification

The second experiment was conducted on a different bearing (Type N205) with a 0.1 mm diameter hole on its outer raceway, The bearing was tested under 1200 rev/min, and the sampling frequency was 20 kHz. As shown in Fig. 17, it is difficult to identify any defect pattern from the raw vibration signal.

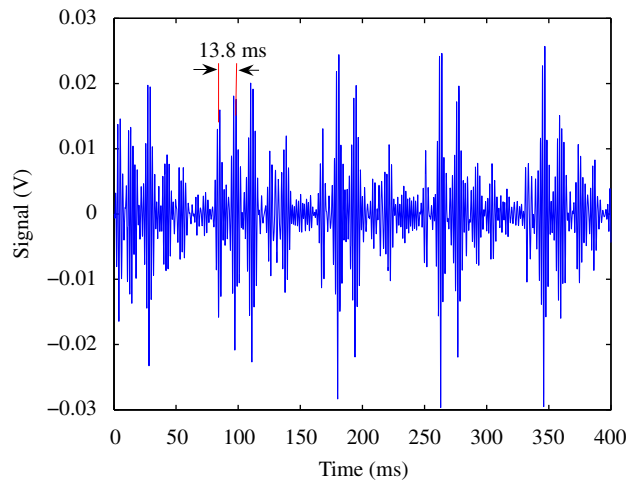


Fig. 15. Filtered results of the bearing vibration signal with harmonic wavelet parameter pair of (800, 1600)Hz.

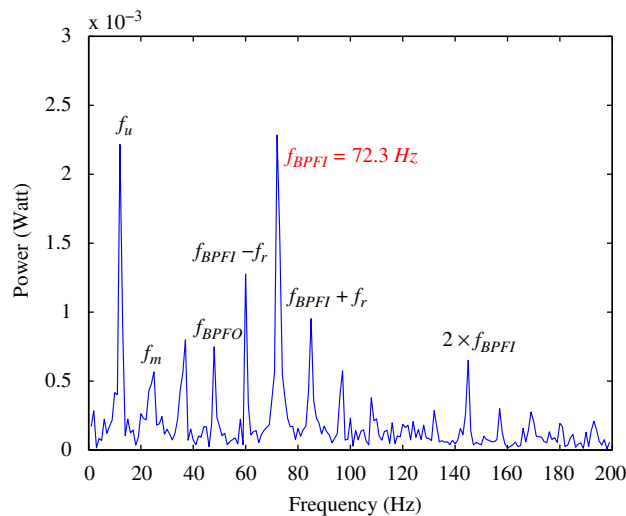


Fig. 16. Enveloping spectrum of the filtered bearing vibration signal with harmonic wavelet parameter pair of (800, 1600)Hz.

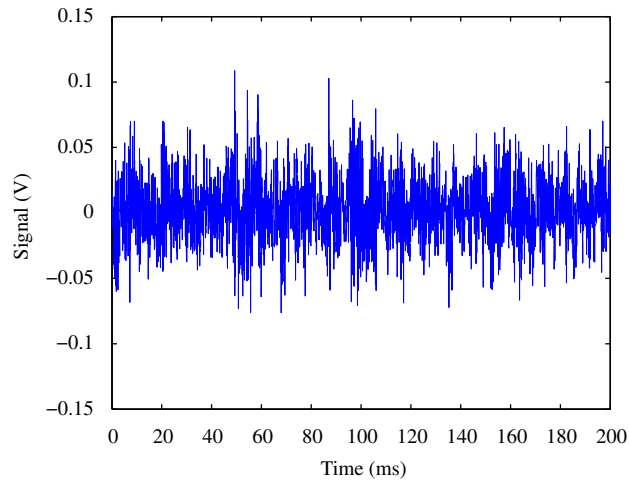


Fig. 17. Signal measured from a type N205 bearing.

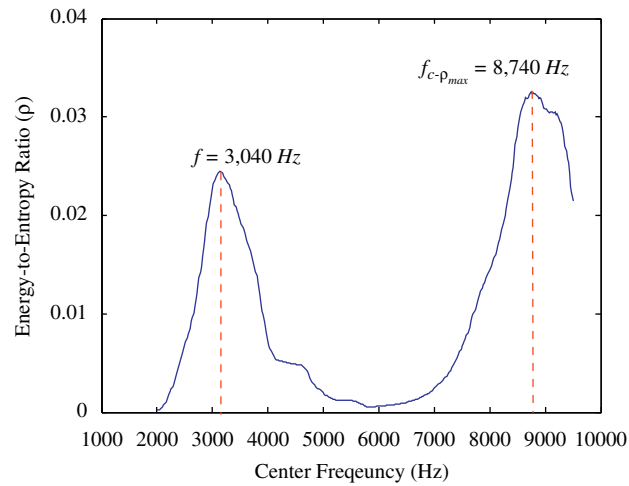


Fig. 18. Energy-to-entropy ratio vs. center frequency.

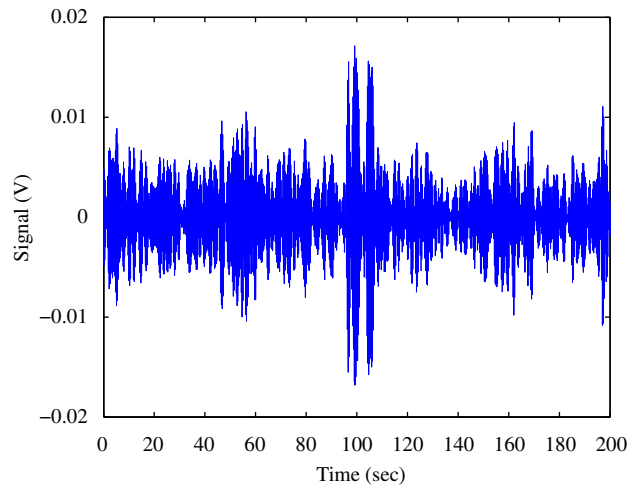


Fig. 19. Filtered results of the bearing vibration signal with harmonic wavelet parameter pair of (2540, 3540) Hz.

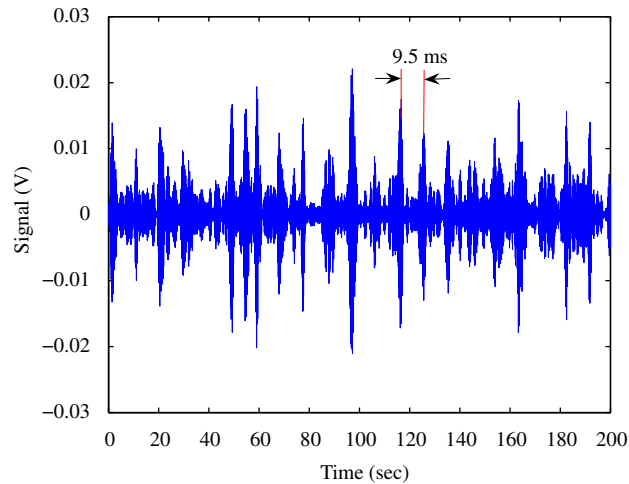


Fig. 20. Filtered results of the bearing vibration signal with harmonic wavelet parameter pair of (8240, 9240)Hz.

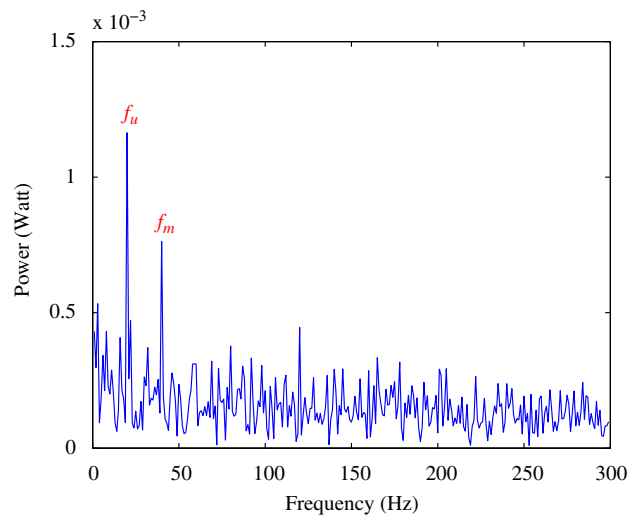


Fig. 21. Enveloping spectrum of the filtered bearing vibration signal with harmonic wavelet parameter pair of (2540, 3540)Hz.

The signal was then analyzed using the harmonic wavelet transform, from which the energy-to-entropy ratio at each of the sub-frequency bands was calculated. As shown in Fig. 18, there are two peaks of energy-to-entropy ratio identified at 3040 and 8740 Hz, respectively. Accordingly, two harmonic wavelet filters can be constructed with the parameter pairs being (2540, 3540) and (8240, 9240) Hz, respectively.

Comparing the filtering results obtained from each of the filters—Fig. 19 from the (2540, 3540) Hz pair and Fig. 20 from the (8240, 9240) Hz pair, it is evident that the (2540, 3540) Hz pair cannot identify any repetitive signal patterns, while the (8240, 9240) Hz pair, which is associated with the highest energy-to-entropy ratio, was able to identify the signal repetition interval of 9.5 ms, which matches the  $f_{\text{BPFO}}=105$  Hz frequency characteristics of the outer raceway defect. As a result, the existence of the outer raceway defect is identified.

This observation is consistent with the enveloping spectrum corresponding to each of the frequency pairs. No defect frequency of  $f_{\text{BPFO}}=105$  Hz is shown to be identified in Fig. 21, which corresponds to the (2540, 3540) Hz pair. In comparison, it is clearly identified in Fig. 22, corresponding to the (8240, 9240) Hz pair.

## 5. Conclusions

A harmonic wavelet transform-based filtering technique is developed for denoising vibration signals measured from rotary machines. Statistical characteristics (i.e. energy and entropy) of the wavelet coefficients are utilized as the basis for selecting the best suited harmonic wavelet parameter pair ( $m, n$ ). The new scheme is computationally efficient, as the

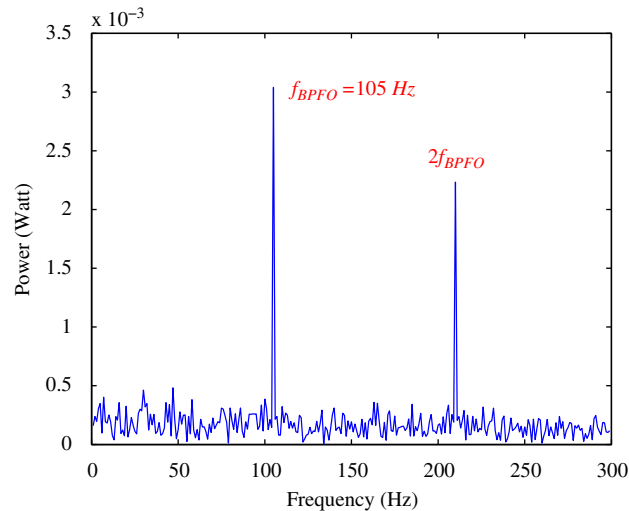


Fig. 22. Enveloping spectrum of the filtered bearing vibration signal with harmonic wavelet parameter pair of (8240, 9240)Hz.

harmonic wavelet transform can be implemented through a compact algorithm based on a pair of Fourier and inverse Fourier transforms. In addition to computational efficiency, the harmonic wavelet filter has also demonstrated better performance than the traditional band-pass filters. A synthetic signal was formulated to quantitatively evaluate the effectiveness of the harmonic wavelet filter, and the result was experimentally verified, by using two different rolling bearings with different type of structural defects. Research is being continued to analyze vibration signals from other rotary machine components, with the aim to establish a systematic approach to rotary machine defect identification.

## Acknowledgements

This work was partly supported by the National Science Foundation under grants CMMI-0218161 and CMMI-0330171. Experimental support provided by the SKF Company is acknowledged.

## References

- [1] M. Meo, G. Zumpano, On the optimal sensor placement techniques for a bridge structure, *Engineering Structures* 27 (2005) 1488–1497.
- [2] S. Sheng, L. Zhang, R. Gao, A systematic sensor-placement strategy for enhanced defect detection in rolling bearings, *IEEE Sensors Journal* 6 (5) (2006) 1346–1354.
- [3] X. Chimentin, F. Bolaers, L. Rasolofondraibe, J.-P. Dron, Localization and quantification of vibratory sources: application to the predictive maintenance of rolling bearings, *Journal of Sound and Vibration* 316 (2008) 331–347.
- [4] J. Sanza, R. Pererab, C. Huerta, Fault diagnosis of rotating machinery based on auto-associative neural networks and wavelet transforms, *Journal of Sound and Vibration* 302 (2007) 981–999.
- [5] W.J. Wang, P.D. McFadden, Application of orthogonal wavelets to early gear damage detection, *Mechanical Systems and Signal Processing* 9 (5) (1995) 497–507.
- [6] S.K. Goumas, M.E. Zervakis, G.S. Stavrakakis, Classification of washing machine vibration signals using discrete wavelet analysis for feature extraction, *IEEE Transactions on Instrumentation and Measurement* 51 (3) (2002) 497–508.
- [7] I. Daubechies, The wavelet transform time–frequency localization and signal analysis, *IEEE Transactions on Information Theory* 36 (5) (1990) 961–1005.
- [8] S. Mallat, *A Wavelet Tour of Signal Processing*, Academic Press, 1999.
- [9] K. Zhu, Y. Wong, H. Soon, Wavelet analysis of sensor signals for tool condition monitoring: a review and some new results, *International Journal of Machine Tools & Manufacture* 49 (2009) 537–553.
- [10] D.E. Newland, *Random Vibrations, Spectral and Wavelet Analysis*, Third ed., Longman, Harlow, John Wiley, New York, 1993.
- [11] S.V. Muniandy, I.M. Moroz, Galerkin modeling of the Burgers equation using harmonic wavelets, *Physics Letters A* 235 (1997) 352–356.
- [12] C. Cattani, Harmonic wavelets towards the solution of nonlinear PDE, *Computers and Mathematics with Applications* 50 (2005) 1191–1210.
- [13] R.A. Bates, M.F. Hilton, K.R. Godfrey, M.J. Chappell, Autonomic function assessment using analysis of heart rate variability, *Control Engineering Practice* 5 (12) (1997) 1731–1737.
- [14] H. Drolon, F. Druaux, A. Faure, Particle shape analysis and classification using the wavelet transform, *Pattern Recognition Letters* 21 (6–7) (2000) 473–482.
- [15] K.M. Iftekharuddin, Harmonic wavelet joint transform correlator: analysis, algorithm, and application to image denoising, *Optical Engineering* 41 (12) (2002) 3307–3315.
- [16] G. Wang, Z. Yan, X. Hu, H. Xie, Z. Wang, Classification of surface EMG signals using harmonic wavelet packet transform, *Physiological Measurement* 27 (2006) 1255–1267.
- [17] D.E. Newland, Wavelet analysis of vibration Part I: theory; Part II: wavelet maps, *Journal of Vibration and Acoustics* 116 (4) (1994) 409–425.
- [18] T. Musha, T. Kumazawa, Instantaneous structural intensity by the harmonic wavelet transform, *Journal of Sound and Vibration* 306 (2007) 377–388.

- [19] J.I. Bonel-Cerdan, J.L. Nikolajsen, Introduction to harmonic wavelet analysis of machine vibrations, *Proceedings of the 1997 International Gas Turbine and Aeroengine Congress and Exposition*, June 2–5, Orlando, FL, Paper 97-GT-58, 1997.
- [20] V.C. Chancey, G.T. Flowers, C.L. Howard, A harmonic wavelets approach for extracting transient patterns from measured rotor vibration data, *ASME Journal of Engineering for Gas Turbines and Power* 125 (1) (2003) 81–89.
- [21] F. Wan, Q. Xu, S. Li, Vibration analysis of cracked rotor sliding bearing system with rotor–stator rubbing by harmonic wavelet transform, *Journal of Sound and Vibration* 271 (2004) 507–518.
- [22] P.D. Samuel, D.J. Pines, D.G. Lewicki, A comparison of stationary and non-stationary metrics for detecting faults in helicopter gearboxes, *Journal of American Helicopter Society* 45 (2000) 125–136.
- [23] B. Liu, Adaptive harmonic wavelet transform with applications in vibration analysis, *Journal of Sound and Vibration* 262 (2003) 45–64.
- [24] R. Bracewell, *The Fourier Transform and Its Applications*, McGraw-Hill, New York, 1999.
- [25] D.E. Newland, Harmonic wavelet analysis, *Proceedings of the Royal Society of London A* 443 (1993) 203–225.
- [26] D.E. Newland, Harmonic and musical wavelets, *Proceedings of the Royal Society of London A* 444 (1994) 605–620.
- [27] T.M. Cover, J.A. Thomas, *Elements of Information Theory*, John Wiley & Sons Inc., 1991.
- [28] P. Duhamel, H. Hollmann, Split-radix FFT algorithm, *Electronic Letters* 20 (1) (1984) 14–16.
- [29] T.H. Cormen, C.E. Leiserson, R.L. Rivest, C. Stein, *Introduction to Algorithms*, The MIT Press, Massachusetts, 2001.
- [30] P.D. McFadden, J.D. Smith, Model for the vibration produced by a single point defect in a rolling element bearing, *Journal of Sound and Vibration* 96 (1) (1984) 69–82.
- [31] R.W. Hamming, *Digital Filters*, Prentice-Hall, New Jersey, 1989.